



**HAL**  
open science

# Interplay between Dual-State and Aggregation-Induced Emission with ESIPT Scaffolds Containing Triphenylamine Substituents: Experimental and Theoretical Studies

Timothée Stoerkler, Gilles Ulrich, Adèle Laurent, Denis Jacquemin, Julien Massue

## ► To cite this version:

Timothée Stoerkler, Gilles Ulrich, Adèle Laurent, Denis Jacquemin, Julien Massue. Interplay between Dual-State and Aggregation-Induced Emission with ESIPT Scaffolds Containing Triphenylamine Substituents: Experimental and Theoretical Studies. *Journal of Organic Chemistry*, 2023, 88 (13), pp.9225-9236. 10.1021/acs.joc.3c00806 . hal-04283010

**HAL Id: hal-04283010**

**<https://cnrs.hal.science/hal-04283010>**

Submitted on 13 Nov 2023

**HAL** is a multi-disciplinary open access archive for the deposit and dissemination of scientific research documents, whether they are published or not. The documents may come from teaching and research institutions in France or abroad, or from public or private research centers.

L'archive ouverte pluridisciplinaire **HAL**, est destinée au dépôt et à la diffusion de documents scientifiques de niveau recherche, publiés ou non, émanant des établissements d'enseignement et de recherche français ou étrangers, des laboratoires publics ou privés.

# **Interplay between Dual-State and Aggregation-Induced Emission with ES IPT Scaffolds Containing Triphenylamine Substituents: Experimental and Theoretical Studies**

Timothée Stoerkler,<sup>[a]</sup> Gilles Ulrich,<sup>[a]</sup> Adèle D. Laurent,<sup>[b]</sup> Denis Jacquemin,<sup>[b][c]\*</sup> and Julien Massue<sup>[a]\*</sup>

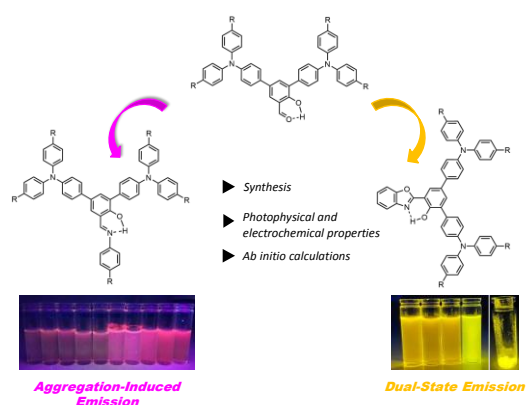
<sup>[a]</sup> Institut de Chimie et Procédés pour l'Énergie, l'Environnement et la Santé (ICPEES), Équipe Chimie Organique pour la Biologie, les Matériaux et l'Optique (COMBO), UMR CNRS 7515, Ecole Européenne de Chimie, Polymères et Matériaux (ECPM), 25 Rue Becquerel, 67087 Strasbourg Cedex 02, France

<sup>[b]</sup> Nantes Université, CNRS, CEISAM UMR 6230, F-44000 Nantes, France

<sup>[c]</sup> Institut Universitaire de France (IUF), F-75005, Paris, France

Emails: [Denis.Jacquemin@univ-nantes.fr](mailto:Denis.Jacquemin@univ-nantes.fr), [massue@unistra.fr](mailto:massue@unistra.fr)

## Abstract



We detail the synthesis of a series of fluorophores containing triphenylamine derivatives, along with their photophysical, electrochemical, and electronic structure properties. These compounds include molecular structures derived from imino-phenol (anil) and hydroxybenzoxazole (HBO) scaffolds originating from similar salicylaldehyde derivatives, and display Excited-State Intramolecular Proton Transfer (ESIPT). We show that depending on the nature of the  $\pi$ -conjugated scaffold, different photophysical processes are observed: Aggregation-Induced Emission (AIE) or Dual-State Emission (DSE), with a modulation of the fluorescence color and redox properties. The photophysical properties are further rationalized with the help of *ab initio* calculations.

## Introduction

Excited-State Intramolecular Proton Transfer (ESIPT) is a four-level photophysical process consisting of a phototautomerization in the electronic excited state, typically converting an enol isomer ( $E^*$ ) into its corresponding keto tautomer ( $K^*$ ), via ultrafast proton transfer (Figure 1a).<sup>1</sup> This phenomenon is typically observed in heteroarenes presenting a strong hydrogen bond in their structure, embedded in five-, six- or seven-membered rings. ESIPT-capable fluorescent dyes are structurally diverse, encompass a wide range of molecular scaffolds<sup>2</sup> and have been applied in all areas of molecular fluorescence, such as optoelectronics,<sup>3</sup> biotechnologies,<sup>4</sup> sensing,<sup>5</sup> security,<sup>6</sup> and others.<sup>7</sup> ESIPT triggers a strong structural reorganization of the molecular scaffold, leading to a fluorescence emission largely redshifted, as compared to the absorption.<sup>8</sup> As a result, fluorophores displaying an ESIPT process are not hampered by self-absorption and inner filter effects, enhancing their photostability over time. A common drawback is, however, the weakly intense emission in solution due to the effective non-radiative decay routes generated by ESIPT, *e.g.*, low-lying Conical Intersection (CI) and Twisted Intramolecular Charge Transfer (TICT) conformations, which can be easily accessed after ESIPT took place. As a result, ESIPT dyes present an unusual behavior as compared to the majority of organic dyes that are typically emissive in solution but strongly quenched in solid, due to Aggregation-Caused Quenching (ACQ) processes. Indeed, due to the restriction of torsional motions in the solid-state, ESIPT dyes have been mainly known as emissive in that state<sup>9</sup> or in aggregates due to their Aggregation-Induced Emission (AIE) property,<sup>10</sup> that are marked when combined with appropriate rotor motifs, such as tetraphenylene,<sup>11</sup> cyanostilbene<sup>12</sup> or specific heterocycles.<sup>13</sup> Nonetheless, it was recently reported that the detrimental molecular motions plaguing fluorescence in solution can be reduced by increasing molecular rigidity<sup>14</sup> or using resonance effects,<sup>15</sup> leading to emission in both solution- and solid-states, *i.e.*, dual-state emission (DSE).<sup>16</sup> We underline that the ESIPT process can be finely modulated or frustrated by the close environment of dyes or their electronic structures. Different situations are encountered, *e.g.*, observation of a full ESIPT process, leading to redshifted  $K^*$  emission, partial frustration of ESIPT process, triggering ratiometric  $E^*/K^*$  dual emission,<sup>17</sup> or full frustration of ESIPT, affording highly solvatochromic push-pull derivatives.<sup>18</sup> Another possibility is a competitive deprotonation process, in the ground or excited state, leading to the presence of highly emissive anionic species.<sup>19</sup> Taking advantage of this modulation of the photophysical properties, numerous examples of stimuli-responsive fluorescent materials based on ESIPT have been engineered.<sup>20</sup>

Although ESIPT fluorescence has become a well-known process, demonstrating rich and modular photophysics, it remains important to design new derivatives with greater synthetic availability, improved properties, and higher versatility. It is particularly essential to gain access to synthetic intermediates which can easily, preferentially in one step, lead to functional ESIPT derivatives with adaptative and responsive optical properties. In this context, we recently developed aryl- and

heteroaryl-substituted imino-phenol (anil) compounds showing a combination of ESIPT and AIE features.<sup>21</sup> These compounds can be obtained in two steps from functionalized salicylaldehydes and 1,4-phenylene diamine and, interestingly, they show a modular pH-sensitive AIE/ESIPT fluorescence color depending on the electronic nature of the substituents.<sup>21</sup> To build on these pioneer results, we decided to investigate salicylaldehyde derivatives, substituted at the 3 and 5 positions by triphenylamine (TPA) moieties. Indeed, it is well-known that many TPA-derived dyes can act as stimuli-responsive solid-state fluorescent materials.<sup>22</sup> Moreover, mono-substituted TPA salicylaldehydes have been recently described to show interesting AIE/ESIPT properties<sup>23</sup> and applied as imaging agents for lipid droplets.<sup>24</sup>

In this article, we report the synthesis, photophysical characterization (solution, solid-state and AIE studies), electrochemical properties and first-principle calculations on a series of ESIPT derivatives either based on a mono-, bis- imino-phenol (anil) or 2-(2'-hydroxyphenyl)benzoxazole (HBO) scaffolds, both known to be ESIPT-capable backbones. Notably, HBO compounds represent an important class of ESIPT dyes and have been intensively studied for their attractive photophysical properties.<sup>25</sup> We show that all these targets derive from 3,5-triphenylamine salicylaldehyde intermediates **salicyl-TPA** and **salicyl-TPA-OMe** (Figure 1b). Depending on the nature of the intermediate but also on the target scaffold, different optical profiles (AIE or DSE) were found, highlighting the versatility of these fluorescent architectures.

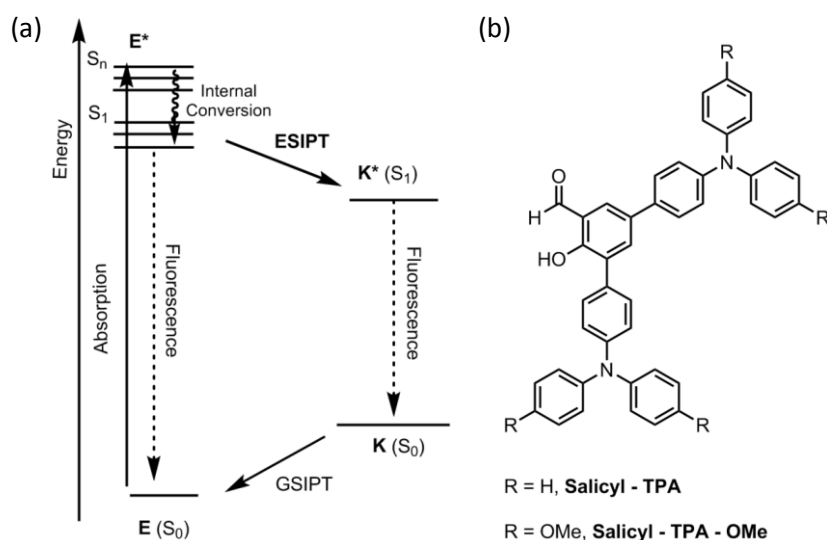


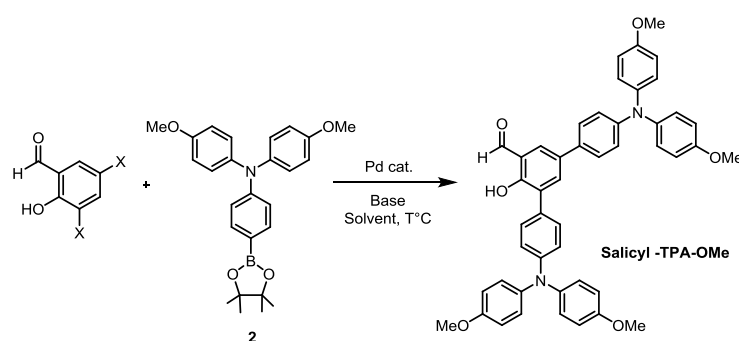
**Figure 1.** (a) Schematic representation of the ESIPT process, involving Enol/Keto ( $E^*/K^*$ ) phototautomerism and (b) Target salicylaldehyde intermediates.

## Results and discussion

### Synthesis

**Salicyl-TPA** was easily synthesized in 91% yield, in one step by Pd-catalyzed Suzuki cross-coupling reaction, from commercially available 3,5-diiodosalicylaldehyde and 4-(diphenylamino)phenyl boronic acid (Scheme S1). **Salicyl-TPA-OMe** was obtained from TPA derivative **2**, which was itself prepared by, first a Pd-catalyzed Buchwald-Hartwig coupling to yield bromo-TPA **1**, followed by the introduction of the dioxaborolane moiety (Scheme S2). **Salicyl-TPA-OMe** was synthesized via a Suzuki cross-coupling reaction between **2** and 3,5-dihalogenosalicylaldehyde. Optimization of the Pd-catalyzed cross-coupling reaction was performed on commercially available 3,5-dihalogenosalicylaldehyde with variations of the catalyst, base, time of reaction and solvent (Table 1).

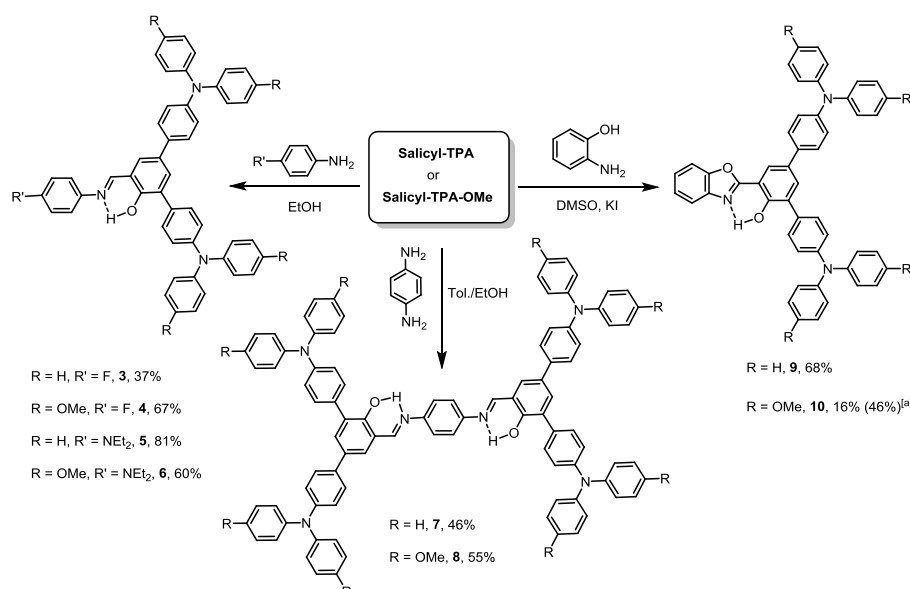
**Table 1.** Optimization conditions for the synthesis of **Salicyl-TPA-OMe**



Entry	X	Cat.	Base	Time (h)	T°C	Solvent	Yield
1	Br	Pd(PPh <sub>3</sub> ) <sub>2</sub> Cl <sub>2</sub>	K <sub>2</sub> CO <sub>3</sub>	12	95°C	dioxane/H <sub>2</sub> O 3:1	22%
2	Br	Pd(PPh <sub>3</sub> ) <sub>2</sub> Cl <sub>2</sub>	K <sub>2</sub> CO <sub>3</sub>	12	95°C	toluene/EtOH 2:1	No reaction
3	Br	Pd(PPh <sub>3</sub> ) <sub>2</sub> Cl <sub>2</sub>	K <sub>2</sub> CO <sub>3</sub>	12	105°C	dioxane/H <sub>2</sub> O 2:1	39%
4	Br	Pd(dppf)Cl <sub>2</sub>	K <sub>2</sub> CO <sub>3</sub>	36	105°C	dioxane/H <sub>2</sub> O 2:1	14%
5	I	Pd(PPh <sub>3</sub> ) <sub>2</sub> Cl <sub>2</sub>	K <sub>2</sub> CO <sub>3</sub> (2M)	12	80°C	dioxane	26%
6	I	Pd(PPh <sub>3</sub> ) <sub>2</sub> Cl <sub>2</sub>	K <sub>2</sub> CO <sub>3</sub> (2M)	12	120°C	toluene	No reaction
7	I	Pd(PPh <sub>3</sub> ) <sub>2</sub> Cl <sub>2</sub>	K <sub>2</sub> CO <sub>3</sub> (2M)	1	105°C	dioxane	10%
8	I	Pd(PPh <sub>3</sub> ) <sub>2</sub> Cl <sub>2</sub>	K <sub>2</sub> CO <sub>3</sub> (2M)	1	125°C	dioxane	5%
9	I	Pd(PPh <sub>3</sub> ) <sub>2</sub> Cl <sub>2</sub>	K <sub>2</sub> CO <sub>3</sub> (2M)	1 then 1	60°C then 90°C	dioxane	7%
10	I	Pd(PPh <sub>3</sub> ) <sub>2</sub> Cl <sub>2</sub>	K <sub>2</sub> CO <sub>3</sub> (2M)	1 then 3	95°C then 110°C	toluene/THF 3:2	No reaction
11	I	Pd(PPh <sub>3</sub> ) <sub>2</sub> Cl <sub>2</sub>	K <sub>2</sub> CO <sub>3</sub> (2M)	1	105°C	dioxane/H <sub>2</sub> O 2:1	37%
12	I	Pd(PPh <sub>3</sub> ) <sub>2</sub> Cl <sub>2</sub>	K <sub>2</sub> CO <sub>3</sub>	2	105°C	dioxane/H <sub>2</sub> O 1:5	15%
13	I	Pd(PPh <sub>3</sub> ) <sub>2</sub> Cl <sub>2</sub>	K <sub>2</sub> CO <sub>3</sub>	12	105°C	dioxane/H <sub>2</sub> O 2:1	57%
14	I	Pd(PPh <sub>3</sub> ) <sub>2</sub> Cl <sub>2</sub>	NH <sub>4</sub> H <sub>2</sub> PO <sub>4</sub>	1	105°C	dioxane/H <sub>2</sub> O 2:1	5%
15	I	Pd(PPh <sub>3</sub> ) <sub>2</sub> Cl <sub>2</sub>	K <sub>2</sub> CO <sub>3</sub>	0.25	105°C	dioxane/H <sub>2</sub> O 2:1	41%
16	I	Pd(PPh <sub>3</sub> ) <sub>2</sub> Cl <sub>2</sub>	K <sub>2</sub> CO <sub>3</sub>	0.5	MW 150°C	dioxane/H <sub>2</sub> O 2:1	45%
17	I	Pd(PPh <sub>3</sub> ) <sub>2</sub> Cl <sub>2</sub>	NH <sub>4</sub> H <sub>2</sub> PO <sub>4</sub>	0.5	MW 150°C	dioxane/H <sub>2</sub> O 2:1	15%
18	I	Pd(PPh <sub>3</sub> ) <sub>2</sub> Cl <sub>2</sub>	K <sub>2</sub> CO <sub>3</sub>	1	MW 150°C	dioxane/H <sub>2</sub> O 2:1	20%
19	I	Pd(PPh <sub>3</sub> ) <sub>2</sub> Cl <sub>2</sub>	K <sub>2</sub> CO <sub>3</sub>	2	MW 150°C	dioxane/H <sub>2</sub> O 2:1	23%
20	I	Pd(dppf)Cl <sub>2</sub>	K <sub>2</sub> CO <sub>3</sub>	12	105°	dioxane/H <sub>2</sub> O 2:1	41%
21	I	Pd(OAc) <sub>2</sub> /Xphos	K <sub>2</sub> CO <sub>3</sub>	12	105°C	dioxane/H <sub>2</sub> O 2:1	31%
22	I	Pd(OAc) <sub>2</sub> /P( <i>o</i> -tol) <sub>3</sub>	K <sub>2</sub> CO <sub>3</sub>	12	105°C	dioxane/H <sub>2</sub> O 2:1	27%

23	I	Pd(PPh <sub>3</sub> ) <sub>2</sub> Cl <sub>2</sub>	Cs <sub>2</sub> CO <sub>3</sub>	12	105°C	dioxane/H <sub>2</sub> O 2:1	64%
24	I	Pd(PPh <sub>3</sub> ) <sub>2</sub> Cl <sub>2</sub>	CsF	12	105°C	dioxane/H <sub>2</sub> O 2:1	55%
25	I	Pd(PPh <sub>3</sub> ) <sub>2</sub> Cl <sub>2</sub>	NaOtBu	12	105°C	dioxane/H <sub>2</sub> O 2:1	33%
26	I	Pd(PPh <sub>3</sub> ) <sub>2</sub> Cl <sub>2</sub>	K <sub>3</sub> PO <sub>4</sub>	12	105°C	dioxane/H <sub>2</sub> O 2:1	29%

During the course of our optimization process, we found out that the nature of the solvents is crucial; notably, the presence of water, seems necessary to obtain reasonable yields of the target salicylaldehyde. A mixture of 1,4-dioxane and water, in 2:1 proportion appeared to be a good compromise between solubility of reagents and reactivity, while the use of toluene led to the absence of reaction. The nature of the base, as well as the temperature seem to play an important role in the achievement of the cross-coupling reaction. Introduction of K<sub>2</sub>CO<sub>3</sub> or Cs<sub>2</sub>CO<sub>3</sub> at a temperature of 105°C led to the best reaction yields (entries 13 and 23 in Table 1). Besides, the nature of the catalyst seems to induce smaller variations of reaction yields (entries 20 and 23). Eventually, the use of PdCl<sub>2</sub>(PPh<sub>3</sub>)<sub>2</sub> as 5% mol. catalyst with cesium carbonate as a base in 1,4-dioxane/water (2/1) led to the preparation of salicylaldehyde **Salicyl-TPA-OMe** in 64% yield, after purification on column chromatography. With the salicylaldehydes **Salicyl-TPA** and **Salicyl-TPA-OMe** in hand, we decided to investigate their one-step reaction with 4-substituted anilines, 1,4-phenylenediamines or 2-aminophenols to obtain a variety of ESIPT-capable structures (Scheme 1). Specifically, the reaction of the starting salicylaldehydes with 4-fluoroaniline or 4-N,N-diethylaminoaniline led to anil derivatives **3-6** in 37-81% yields, and with 1,4-phenylene diamine afforded bis-anils **7** and **8** in 46 and 55 % yield, respectively. We highlight that these condensations took place in toluene/ethanol mixtures and that the desired products were collected by simple filtration.



**Scheme 1.** Synthesis of anils **3-6**, bis-anils **7, 8** and HBO **9, 10**. <sup>[a]</sup> MeOH/DMSO (9:1, v/v), KCN, ArB(OH)<sub>2</sub>, RT.

Condensation of **Salicyl-TPA** with 2-aminophenol in the presence of potassium iodide at 110°C in DMSO allowed the formation of HBO dye **9** in 68% yield. However, condensation of **Salicyl-TPA-OMe** following the same protocol only yielded target product HBO **10** in 16% yield. This low yield could be due to instability issues of electron-rich TPA-OMe moieties at high temperatures. As a result, smoother reaction conditions were tested, with the presence of potassium cyanide and phenyl boronic acid in a mixture of DMSO and methanol at room temperature.<sup>17a</sup> Following this route, **10** was obtained in 46% yield (see experimental section).

### Photophysical properties

First, the photophysical properties of all targets were recorded in THF solution, at room temperature and 77K for anils **3-6** and bis-anils **7** and **8**, and in multiple solvents for HBO **9** and **10**, as well as in the solid-state as powders. The results are given in Table 2, whereas the absorption spectra of all dyes can be seen in Figures 2 and S19-S24, while the emission spectra are presented on Figures 3a-c, S21-22 and S29.

**Table 2.** Photophysical data in aerated solutions at 25°C and in the solid-state as amorphous powders.

Dye	Solvent	$\lambda_{\text{abs}}$ [a] (nm)	$\epsilon \times 10^{-3}$ ( $M^{-1} \cdot \text{cm}^{-1}$ )	$\lambda_{\text{em}}$ [b] (nm)	$\Delta\text{SS}^{[c]}$ ( $\text{cm}^{-1}$ )	$\lambda_{\text{em}}$ [d] (nm)	QY <sup>[e]</sup>	$\tau$ (ns)
<b>Anil 3</b>	THF	319, 403	65.5/8.2	<sup>[f]</sup> (655) <sup>[g]</sup>	-	624	-	-
	Solid	463	-	658	6400	-	0.01	-
<b>Anil 4</b>	THF	326, 415	55.6/7.2	<sup>[f]</sup> (655) <sup>[g]</sup>	-	645	-	-
	Solid	468	-	657	6100	-	0.01	-
<b>Anil 5</b>	THF	311, 402	64.3/30.8	629 (639) <sup>[g]</sup>	9000	628	0.02	0.3
	Solid	470	-	637	5600	-	0.01	-
<b>Anil 6</b>	THF	335, 392	45.3/28.8	642 (648) <sup>[g]</sup>	10000	645	0.01	0.6
	Solid	469	-	654	6000	-	0.01	-
<b>Bis-anil 7</b>	THF	332, 426	100.9/21.4	<sup>[f]</sup> (671) <sup>[g]</sup>	-	661	-	-
	Solid	468	-	672	6100	-	0.01	-
<b>Bis-anil 8</b>	THF	337, 430	107.1/17.5	<sup>[f]</sup> (673) <sup>[g]</sup>	-	698	-	-
	Solid	467	-	684	6800	-	0.01	-
<b>HBO 9</b>	Toluene	309, 372	67.3/13.9	577	8600	-	0.06	2.0
	CH <sub>2</sub> Cl <sub>2</sub>	308, 384	58.8/10.2	578	9700	-	0.08	1.2
	THF	308, 378	62.0/12.4	578 (570) <sup>[g]</sup>	9600	562	0.12	1.2
	DMF	304, 381	71.9/12.8	526	5000	-	0.25	5.0
	Solid	411	-	562	6500	-	0.25	-
<b>HBO</b>	Toluene	317, 402	40.8/7.8	584	8600	-	0.13	1.5

<b>10</b>	CH <sub>2</sub> Cl <sub>2</sub>	315, 394	59.3/11.0	589	9000	-	0.10	3.0
	THF	329, 395	54.8/10.4	586 (570) <sup>[g]</sup>	8500	585	0.09	1.6
	DMF	320, 389	52.8/10.5	553	7200	-	0.08	5.2
	Solid	431	-	565	5500	-	0.18	-

<sup>[a]</sup> Absorption wavelength in THF solution ( $C = 10^{-5} M$ ), <sup>[b]</sup> Emission wavelength at 25°C ( $C = 10^{-6} M$  for solution measurements), <sup>[c]</sup> Stokes' shift in solution, <sup>[d]</sup> Emission wavelength in aggregated state, in THF/H<sub>2</sub>O 10/90 at 25°C <sup>[e]</sup> Quantum yield in solution, using Rhodamine 6G as a reference ( $\lambda_{exc} = 488 \text{ nm}$ ,  $\Phi = 0.88$  in ethanol); Quantum yield in the solid-state, as absolute (calculated with an integration sphere), <sup>[f]</sup> Not fluorescent, <sup>[g]</sup> Recorded at 77k.

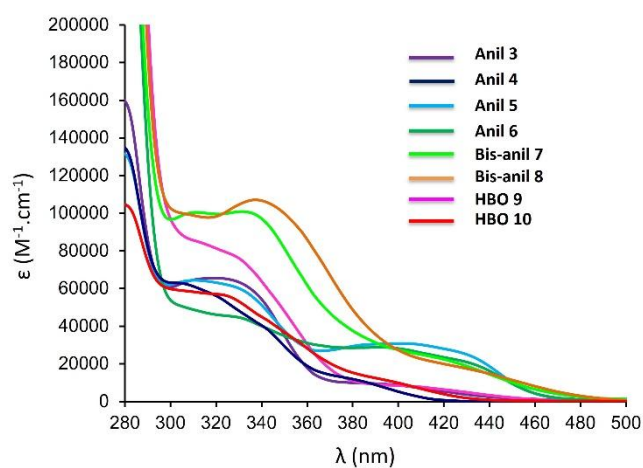


**Figure 2.** Absorption spectra of all dyes in THF. Concentration 10 $\mu$ M.

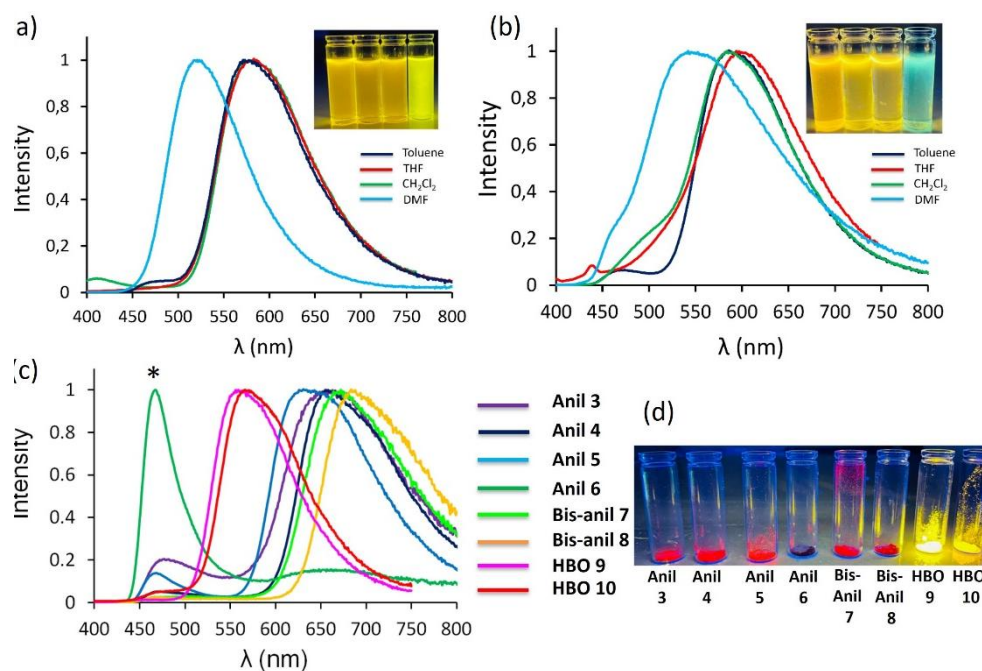


**Figure 3.** Emission spectra of (a) HBO 9 and (b) HBO 10 in toluene (navy blue), dichloromethane (green), THF (red) and DMF (blue) ( $\lambda_{\text{exc}} = 380$  nm), along with photographs of solutions in toluene, dichloromethane, THF and DMF (insets, left to right) under irradiation ( $\lambda_{\text{exc}} = 365$  nm). (c) Emission spectra in the solid-state as powders ( $\lambda_{\text{exc}} = 390$  nm) for anils 3 (purple), 4 (navy blue), 5 (blue), 6 (green), 7 (light green), 8 (orange) and HBO 9 (pink) and 10 (red), (d) photographs of compounds 3-10 (left to right), under irradiation ( $\lambda_{\text{exc}} = 365$  nm), \* denotes oxidized species.

In dilute THF solutions, all dyes display intense high-energy absorption bands located between 302 to 344 nm, with absorption coefficients spanning 45,000-107,000  $\text{M}^{-1}\cdot\text{cm}^{-1}$ , assigned to  $\pi\text{-}\pi^*$  transitions. A second low-energy absorption band is also observed with lower epsilon values ( $\lambda_{\text{abs}} = 378\text{-}430$  nm,  $\epsilon = 7,200\text{-}30,800$   $\text{M}^{-1}\cdot\text{cm}^{-1}$ ) and this band involves a significant charge-transfer character (see calculations below). Subtle differences can be observed in the maximum absorption wavelengths, where the introduction of methoxy groups on triphenylamine moieties leads to small bathochromic shifts. After photoexcitation in the  $S_0\text{-}S_1$  transition, in THF, concerning the anil and bis-anil derivatives 3-8, only those substituted with  $\text{NEt}_2$ , *i.e.*, 5 and 6 display an observable red fluorescence ( $\lambda_{\text{em}} = 629$  and 642 nm) which remains however weak (QY = 2 and 1%, respectively) (Figures S21-S22). It is important to note that the starting salicylaldehydes **Salicyl-TPA** and **Salicyl-TPA-OMe** did not display any observable emission at room temperature (absorption can be seen in Figures S23-S24). However, in frozen solutions at 77K, all dyes show recordable fluorescence, evidencing the importance of rotations in solution in the generation of non-radiative deactivations (Figure S29). Concerning the HBO dyes 9 and 10, they clearly stand out in the series as they display intense

fluorescence in multiple solvents (Figure 3a-b). In toluene, dichloromethane and THF, one finds highly similar emission bands ( $\lambda_{em} = 577\text{-}578$  nm for **9** and  $\lambda_{em} = 584\text{-}586$  nm for **10**) with QY in the range 6-12% and 9-13% for **9** and **10**, respectively. The presence of additional methoxy groups in HBO **10** triggers a mild bathochromic shift in emission. Therefore, in all cases a single not fluorosolvatochromic emission band is observed, consistent with a decay of the  $K^*$  tautomer formed after ESIPT, which is consistent with theory (see below). In dissociative DMF, a blueshift is observed for both dyes ( $\lambda_{em} = 526$  and  $553$  nm for **9** and **10**, respectively), corresponding to a spontaneous deprotonation in the excited-state; a competitive process already observed in the HBO series.<sup>19,26</sup> The fluorescent lifetimes are all in the nanosecond range, following a mono-exponential decay, which are typical values for organic short-lived fluorescence. It is also noteworthy that all dyes display detectable emission in the solid-state, as amorphous powders under irradiation (Figure 3d). Anils and bis-anils dyes **3-8** display emission in solid in the range 637-684 nm with low quantum yields around 1%. In the case of anil **6**, a low-energy emission band, around 460 nm is observed and can be ascribed to the spontaneous formation of unstable oxidized species. This feature, also observed though less clearly, in the case of **5** can be explained by the rich electronic nature of these species owing to the simultaneous presence of TPA and  $NEt_2$  moieties. Open air oxidation can be also visually detected, as shown on Figure 3d where anil **6** appears as a dark powder under irradiation. This strong sensitivity of **6** to oxygen is also highlighted by measuring its electrochemical properties (see below). In contrast, HBO dyes **9** and **10** display bright solid-state emission at 562 and 565 nm, with respective quantum yields of 25 and 18%. It is worth noting that in all cases when fluorescence is observed, in solution or solid, the maximum emission wavelength is only mildly sensitive to the additional presence of methoxy groups on TPA derivatives. Nonetheless, the photophysical studies highlight: 1) strong non-radiative deactivations in the case of all anil/bis-anil dyes **3-7** leading to a marked quenching of fluorescence, and 2) the DSE nature for HBO dyes **9** and **10**, which show significant fluorescence intensity both in solution and in solid. For these two compounds, it is also worth noticing that the anionic species, formed after deprotonation in the excited-state, are also fluorescent, as evidenced in DMF.

### AIE studies

As previous examples in the literature demonstrate the AIE nature of anil derivatives,<sup>21,27</sup> we decided to investigate the formation of aggregates for all dyes in THF/ $H_2O$  mixtures, with a concentration of around  $10\ \mu\text{M}$  (Figure 4 and S21-24).

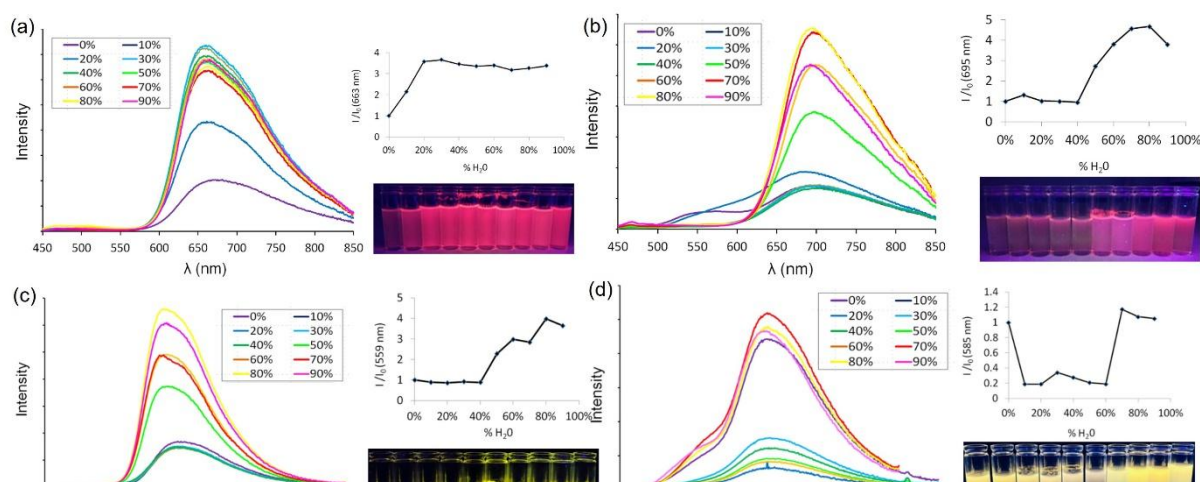


**Figure 4.** AIE behavior in THF/H<sub>2</sub>O mixtures (0% to 90% H<sub>2</sub>O) for (a) bis-anil **7**, (b) bis-anil **8**, (c) HBO **9** and (d) HBO **10**, at 25°C (0%, purple; 10%, black, 20%, navy blue; 30%, blue; 40%, green; 50%, light green; 60%, orange; 70%, red; 80%, yellow; 90%, pink) ( $\lambda_{\text{exc}} = 390$  nm). Insets: Photographs of THF solution with increasing  $f_w$  ( $\lambda_{\text{exc}} = 365$  nm).

As a general observation, all dyes display significant fluorescence intensity enhancement upon addition of water in THF solutions, ascertaining their AIE behavior, to an extent depending on the molecular structure. Being completely quenched or faintly fluorescent in dilute THF solution, mono-anils derivatives **3-6** all display one main emission band, upon gradual addition of water (Figures S21-S24). This band, in the range 624-645 nm can be safely attributed to the decay of the K\* excited tautomer, generated upon ESIPT process. It is worth noting that methoxy-TPA derivatives **4** and **6** show a marked redshift of 20 nm, as compared to unsubstituted TPA **3** and **5**; this redshift being more pronounced for aggregates than in the solid-state (Figure 3c). Additionally, a second emission band is observed for anils **3**, **4**, and **6**, in the higher energies ( $\lambda_{\text{em}} = 466-476$  nm), which could be tentatively attributed to the stabilization of the E\* state, owing to the presence of electronegative fluorine atoms for the first two anils and electron-rich TPA-OMe moieties in the last example. Subtle electronic effects have indeed been evidenced as possible sources of ESIPT partial frustration on related non-AIE examples.<sup>17</sup> It is also clear that a possible instability due to the partial or complete oxidation of the TPA groups, such as the one observed in solid for **6** cannot be ruled out. Bis-anils **7** and **8** also display AIE features, with the appearance of a single band centered at 661 and 698 nm, emphasizing again the influence of the methoxy groups on the red-shifted emission of **8**. In the case of **7**, the increase of emission intensity upon addition of water is fast, reaching a plateau at a water fraction ( $f_w$ ) of 20%, whereas for bis-anil **8**, no evolution of fluorescence is observed below  $f_w$  of 40%. Significant intensity enhancement is then observed up to  $f_w = 80\%$ , where a slight precipitation process likely occurs, causing fluorescence intensity to decrease. We note that, similar to our previous studies on AIE-displaying bis-anil derivatives (lacking TPA groups),<sup>21</sup> only a single EK\* band is observed, meaning the proton transfer of one imino-phenol unit impedes the possibility of a second ESIPT process; a feature consistent with previous *ab initio* calculations on similar systems.<sup>21</sup> Also, we underline that the addition of water does not seem to stabilize E\* emission, unlike many non-AIE ESIPT dyes where protic solvents lead its H-bonded stabilization.<sup>1</sup> The formation of aggregates upon addition of water in the AIE process limits the possibility of partial frustration of the ESIPT process with solvation. The

anils AIEgens **3-8** display a fine-tuning of the maximum emission wavelength, with fluorescence color in the range 624-698 nm, depending on the electronic substitution. Concerning HBO dyes **9** and **10**, they also display AIE properties with maximum emission wavelengths of the aggregates at 562 and 585 nm, respectively. This represents a significant blueshift, as compared to the anils and bis-anils **3-8** derivatives, and provides an easy access to aggregates with a panel of fluorescence colors, starting from the same salicylaldehyde intermediates. All aggregates were also studied with Dynamic Light Scattering (DLS) analysis in THF/H<sub>2</sub>O (9:1) (Figures S36-S42). All dyes show formation of aggregates with the notable exception of **5**, with average particle size in the range 70-100 nm.

#### Electrochemical Properties

To shed additional light on these compounds, cyclic voltammetry was performed on all ESIPT dyes **3-10**, to investigate their oxidation and reduction potential in CH<sub>2</sub>Cl<sub>2</sub> solutions, using *n*-Bu<sub>4</sub>NPF<sub>6</sub> as the supporting electrolyte and ferrocene (Fc) as a reference (Figure 5). Electrochemical data are provided in Table 3.

**Table 3.** Electrochemical data for compounds **3-10**, in CH<sub>2</sub>Cl<sub>2</sub>, at 25°C.

Dye	E <sub>ox</sub> 1 <sup>[a]</sup>	E <sub>red</sub> 1 <sup>[b]</sup>	E <sub>1/2</sub>	E <sub>ox</sub> 2 <sup>[a]</sup>	E <sub>red</sub> 2 <sup>[b]</sup>	E <sub>1/2</sub>	E <sub>ox</sub> 3 <sup>[a]</sup>	E <sub>red</sub> 3 <sup>[b]</sup>	E <sub>1/2</sub>	E <sub>ox</sub> 4 <sup>[a]</sup>	E <sub>red</sub> 4 <sup>[b]</sup>	E <sub>1/2</sub>	E <sub>ox</sub> 5 <sup>[a]</sup>	E <sub>red</sub> 5 <sup>[b]</sup>	E <sub>1/2</sub>
Anil 3	1.255	1.005	0.125	1.515	1.355	0.08	-	-	-	-	-	-	-	-	-
Anil 4	1.05	0.86	0.095	1.4	1.28	0.06	1.83	1.69	0.07	-	-	-	-	-	-
Anil 5	1.015	[c]	[c]	1.105	1.015	0.045	1.265	1.095	0.085	1.385	[c]	[c]	1.515	1.355	0.08
Anil 6	0.965	0.785	0.090	1.125	[c]	[c]	1.445	[c]	[c]	1.715	[c]	[c]	-	-	-
Bis-anil 7	1.040	0.950	0.045	1.25	1.14	0.055	1.52	[c]	[c]	-	-	-	-	-	-
Bis-Anil 8	0.775	0.565	0.105	1.105	[c]	[c]	1.265	[c]	[c]	1.565	[c]	[c]	1.805	[c]	[c]
HBO 9	1.335	1.125	0.105	1.555	1.355	0.1	-	-	-	-	-	-	-	-	-
HBO 10	1.04	0.94	0.05	1.59	1.52	0.035	1.8	1.63	0.085	-	-	-	-	-	-

Potentials are given in V vs Fc/Fc<sup>+</sup> as internal reference and converted to SCE assuming that E<sub>1/2</sub>(Fc/Fc<sup>+</sup>) = +0.38 V (vs SCE). <sup>[a]</sup> E<sub>ox</sub> = Oxidation potential. <sup>[b]</sup> E<sub>red</sub> = Reduction potential. <sup>[c]</sup> Irreversible wave.

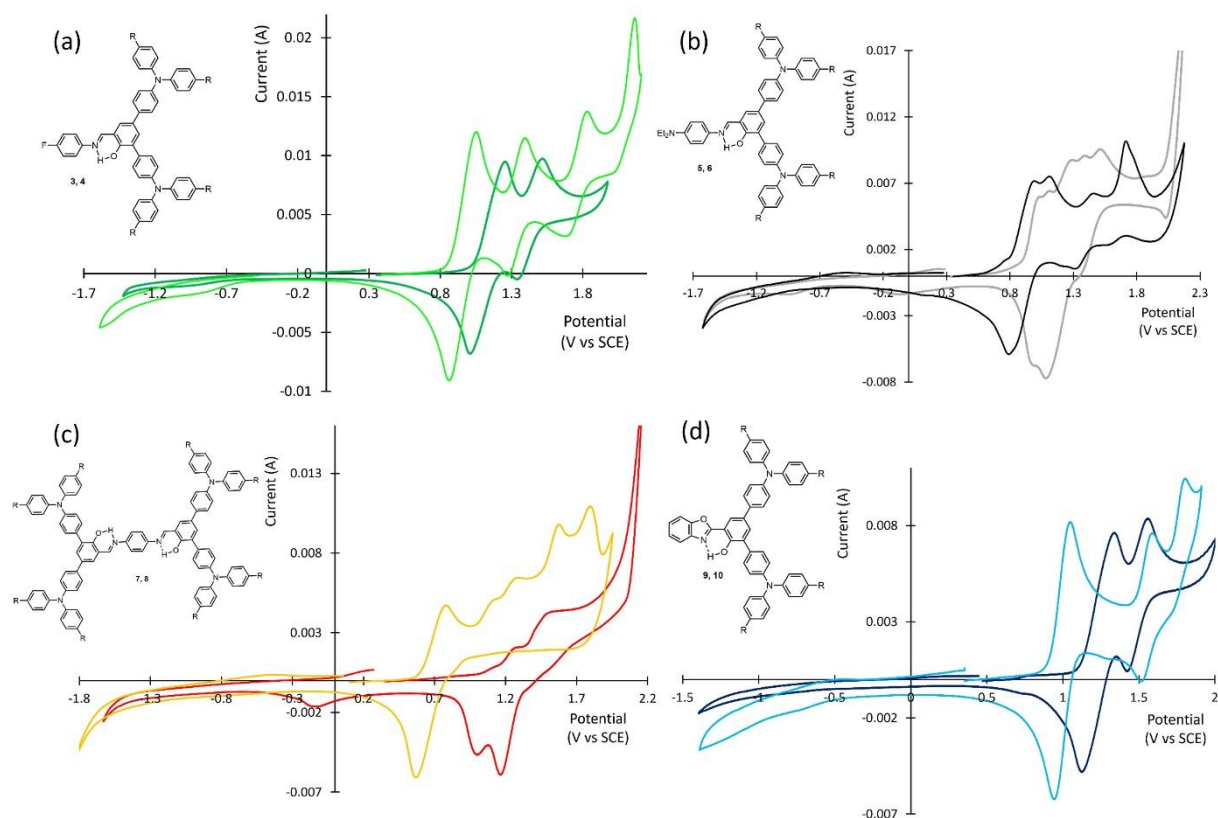


**Figure 5.** Cyclic voltammograms in  $\text{CH}_2\text{Cl}_2$  (with 0.1 M  $\text{Bu}_4\text{NPF}_6$ , as the supporting electrolyte) of a) Anils **3** (green) and **4** (light green), b) Anils **5** (grey) and **6** (black), c) Bis-anils **7** (red) and **8** (orange) and d) HBO **9** (navy blue) and **10** (blue). Recorded with a platinum working electrode. Silver wire was used as an external reference electrode and a platinum wire was used as auxiliary electrode. Ferrocene was used as an internal reference. All cyclic voltammograms were carried out at a scan rate of  $100 \text{ mV s}^{-1}$  with a concentration of analyte of  $1 \text{ mM}$ . The direction of scan is oxidative (starting point 0 V). CVs are plotted using the IUPAC convention and shown between  $-2.0$  and  $2.0 \text{ V}$ .

All compounds exhibit one to five redox processes, reversible or not depending on their molecular structures. In details, anils **3**, **4** and HBO **9**, **10** display a first reversible oxidation wave in the range  $1.04\text{-}1.335 \text{ V}$ , attributed to the simultaneous monoelectronic oxidation of the TPA moieties into radical cations. A second reversible oxidation wave is also observed at potentials  $1.40\text{-}1.59 \text{ V}$ , attributed to a second oxidation of one radical cation into the corresponding dication species. In the case of compounds with TPA-OMe units **4** and **10**, a third irreversible oxidation wave is recorded at  $1.83$  and  $1.80 \text{ V}$ , respectively which likely corresponds to the oxidation of the second TPA groups into dications. It is worth noting that dyes, functionalized with TPA-OMe group show a marked more positive oxidation potential than their unsubstituted-TPA counterparts, owing to the presence of the electron rich methoxy moiety. Anils **5**, **6** and bis-anils **7**, **8** display more complex voltammograms, owing to the presence of multiple redox moieties within their structure, *i.e.*,  $\text{NEt}_2/\text{TPA}$  for the former and four TPA units for the latter. In particular, anil **6** displays one reversible oxidation wave, followed

by three irreversible ones. Moreover, its first oxidation wave can be found at 0.965 V, which is the second-lowest in the series and which can be accountable for the low open-air stability of this compound.

### *Ab initio Calculations*

Using a level of theory combining second-order CC (CC2) calculations<sup>28</sup> and Time-Dependent Density Functional Theory (TD-DFT) that is detailed in the SI,<sup>29</sup> we have modelled the excited-state properties of anils **3-6** and HBO dyes **9** and **10**. The bis-anil derivatives **7** and **8** are unfortunately beyond computational reach at CC2 level. We stress that the selected protocol accounts for both linear-response and state-specific solvation (THF) effects, which is often crucial for ESIPT dyes.<sup>30</sup> Let us start by discussing some quantitative results listed in Table 4. While we are well aware of the limits of the vertical approximation when comparing measured and computed absorption spectra, one can satisfactorily find that the mean absolute deviation between the experimental and measured wavelength is less than 10 nm, with globally satisfying trends.

For **Anils 3-6**, the TD-DFT optimizations of  $E^*$  either predict a direct proton transfer leading to  $K^*$  (for the two former), or to a conical-intersection-like structure (for the two latter). In any case, theory therefore strongly hints that only the keto tautomer can possibly emit in these compounds, with vertical emission energies reasonably close to experiment when comparison is possible (see Tables 2 and 4). For HBO **9**, there is a small driving force for ESIPT to take place in the two solvents (-0.05 eV), and the theoretical fluorescence value determined for the  $K^*$  tautomer clearly better fits the experimental outcomes, so ESIPT clearly takes place in that compound.

In DMF, we computed the emission of the anion (which is bright with a large oscillator strength) at 514 nm, in between the one of the enol and keto form, which is consistent with the measurements (526 nm) For its methoxy substituted form, **HBO 10**, the theoretical results are more contrasted, but comparing all values indicates that ESIPT likely takes place in that compound as well. To obtain a more qualitative picture of the electronic transitions, we provide in Figure 6, electron density difference (EDD) representations for selected dyes (further data can be found in the ESI). In all cases, one finds the usual topology for ESIPT dyes, with a loss of electron density and hence an increase of acidity for the phenolic functional group, and the reverse behavior for the proton-accepting group. One also notices the clear donating character of the amino groups, albeit with a strong difference between anils **3** and **5**. In the former, there is charge-transfer from the TPA units to the dye core, whereas in the latter, the CT takes place from the diethylamino group, positioned on the imino side towards the core; the two TPA units having a passive role as they are slightly twisted compared to the anil core. This notable difference could be one the sources of the different behaviors of the two series of anils, **3-4** and **5-6** in solution and in the solid-state.

**Table 4.** Computed photophysical properties for selected dyes. We report the vertical absorption and emission energies in nm, considering the various possible forms for the latter (see text), as well as the energy difference between the keto and enol forms in the excited state (in eV, a negative value indicates a more stable K\* tautomer. For the latter both TD-DFT and CC2-corrected values are displayed, whereas all transition wavelengths include CC2 corrections. In DMF we also computed the emission of the anion.

Dye	Solvent	$\lambda_{\text{vert-abs}}$ (nm)	$\lambda_{\text{vert-fl E}^*}$ (nm)	$\lambda_{\text{vert-fl K}^*}$ (nm)	$\lambda_{\text{vert-fl A}^*}$ (nm)	$\Delta E^{\text{TD-DFT}}$ (eV)	$\Delta E^{\text{CC2}}$ (eV)
Anil 3	THF	383	[a]	635	-	-	-
Anil 4	THF	403	[a]	655	-	-	-
Anil 5	THF	399	[a]	607	-	-	-
Anil 6	THF	403	[a]	627	-	-	-
HBO 9	THF	365	447	559	-	-0.09	-0.05
HBO 9	DMF	365	451	558	514	-0.10	-0.05
HBO 10	THF	383	508	578	-	-0.02	+0.04

[a] Enol form unfound (see main text)

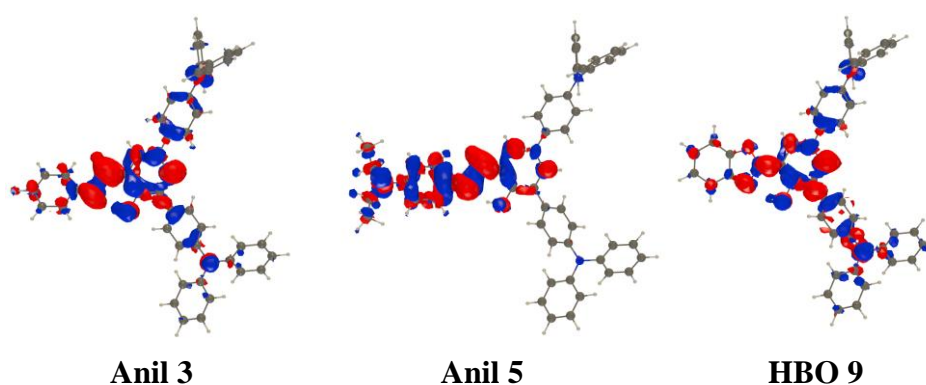


**Figure 6.** Density difference plot corresponding to the absorption from the ground-state. The blue and red lobes represent decrease and increase of electron density upon absorption. Contour: 0.001

## Conclusions

We have designed, synthesized and fully characterized a whole series of fluorophores derived from similar salicylaldehyde intermediates and showing ESIPT. Two different scaffolds were constructed: imino-phenols (anils) and HBO dyes, functionalized with triphenylamino- or 4-methoxytriphenylamino- moieties. Photophysical investigations revealed different optical behaviors; for the former case, strong fluorescence quenching in the molecular state and subsequent AIE features are observed, while in the latter case, dual solution- and solid-state emissions, along with AIE properties were observed. Moreover, the fluorescence color can be easily fine-tuned by the electronic

substitution, without significantly altering neither the AIE, nor the ESIPT process. Electrochemical data shed additional light on the advantage of the introduction of TPA-OMe groups in lieu of TPA, in terms of modular oxidation potentials. Finally, *ab initio* calculations rationalized the nature of the transitions involved in the radiations observed. Future development will focus on inserting these emissive materials in optoelectronic devices.

**Keywords:** Triphenylamine - ESIPT- Aggregation-induced Emission - Fluorescence- *ab initio* calculations

## Experimental section

TPA derivatives **1**<sup>31</sup> and **2**<sup>32</sup> were prepared, following reported procedures.

### Synthesis of Salicyl-TPA<sup>33</sup>

3,5-diiodosalicylaldehyde (0.1 mmol.), 4-(diphenylamino)phenyl boronic acid (0.3 mmol.), potassium carbonate (0.4 mmol.) and bis(triphenylphosphine)palladium(II) dichloride (5 mol%) are dried under vacuum for five minutes in a Schlenk tube and put under argon atmosphere. 1,4-dioxane/H<sub>2</sub>O (2/1) was degassed with argon for 15 minutes and added to the solids via cannula. The resulting mixture was stirred for 15 hours at room temperature, in the sealed schlenk tube, before it was quenched with saturated NH<sub>4</sub>Cl. The yellow precipitate was filtered on a sintered funnel, washed with water, before it was filtered through a silica pad eluting with chloroform. The solvent was removed *in vacuo* to afford **Salicyl-TPA** as a yellow powder (128 mg, 91 %). Mp 284 - 286 °C. <sup>1</sup>H NMR (400 MHz, CDCl<sub>3</sub>) δ 11.54 (s, 1H), 10.01 (s, 1H), 7.84 (d, <sup>4</sup>J = 2.3 Hz, 1H), 7.70 (d, <sup>4</sup>J = 2.3 Hz, 1H), 7.53 (d, <sup>3</sup>J = 8.7 Hz, 2H), 7.47 (d, <sup>3</sup>J = 8.7 Hz, 2H), 7.31-7.24 (m, 8H), 7.18-7.10 (m, 12H), 7.07-7.01 (m, 4H). HRMS (ESI-TOF) m/z: [M+H] Calcd for C<sub>43</sub>H<sub>32</sub>N<sub>2</sub>O<sub>2</sub>: 608.2458, Found: 608.2446. IR (neat): ν = 3444, 2925, 2854, 1733, 1685, 1454, 1375, 1309, 1119, 833, 743, 703 cm<sup>-1</sup>.

### Suzuki-Miyaura Cross-Coupling Reaction Conditions on 3,5-dihalogenosalicylaldehyde.

In a Schlenk tube, 3,5-dihalogenosalicylaldehyde (0.1 mmol), TPA **2** (0.3 mmol), and base (0.4 mmol) were dissolved in a solvent (45 mL/mmol). The resulting suspension was degassed with argon before the addition of the catalyst (5% mol). After a given time of stirring at a given temperature, using an oil bath, the crude product was analyzed by <sup>1</sup>H NMR.

### Synthesis of Salicyl-TPA-OMe

3,5-diiodosalicylaldehyde (0.1 mmol.), TPA **2** (0.3 mmol.), cesium carbonate (0.4 mmol.) and bis(triphenylphosphine)palladium(II) dichloride (5 mol%) are dried under vacuum for five minutes in a Schlenk tube and put under argon. 1,4-dioxane/H<sub>2</sub>O (2/1) was degassed with argon for 15 minutes and added to the solids via cannula. The resulting mixture was stirred for 15 hours at 105°C in the sealed schlenk tube, before it was allowed to cool down to room temperature. The crude mixture was then filtered through a silica plug washing with dichloromethane. The organic phase was acidified

with a concentrated  $\text{NH}_4\text{Cl}$  solution, washed with water and brine, dried on  $\text{MgSO}_4$  before the solvents were removed *in vacuo*. Purification by chromatography on silica gel, eluting with Pet. Ether/AcOEt (10/0 to 8/2) afforded **Salicyl-TPA-Ome** as a yellow powder. (108 mg, 64%). Mp 85 - 90 °C (degradation).  $^1\text{H}$  NMR (500 MHz,  $\text{CDCl}_3$ )  $\delta$  11.49 (s, 1H), 9.99 (s, 1H), 7.79 (d,  $^4J = 2.3$  Hz, 1H), 7.64 (d,  $^4J = 2.3$  Hz, 1H), 7.46 (d,  $^3J = 8.7$  Hz, 2H), 7.39 (d,  $^3J = 8.7$  Hz, 2H), 7.14-7.05 (m, 8H), 7.01-6.96 (m, 4H), 6.87-6.82 (m, 8H), 3.81 (s, 6H), 3.80 (s, 6H).  $^{13}\text{C}\{^1\text{H}\}$  NMR (126 MHz,  $\text{CDCl}_3$ )  $\delta$  197.2, 157.8, 156.1, 156.1, 148.5, 148.4, 140.9, 140.9, 135.8, 133.2, 131.4, 130.7, 130.0, 130.0, 128.0, 127.0, 127.0, 126.8, 121.1, 120.9, 119.9, 114.9, 114.9, 55.6. HRMS (ESI-TOF) m/z: [M+H] Calcd for  $\text{C}_{47}\text{H}_{40}\text{N}_2\text{O}_6$ : 728.2881, Found: 728.2839. IR (neat):  $\nu = 3036, 2928, 2832, 1650, 1604, 1497, 1318, 1274, 1232, 1176, 1105, 1030, 822, 763, 573, 521$   $\text{cm}^{-1}$ .

### General procedure for the synthesis of anils 3-6 and bis-anils 7, 8

**Salicyl-TPA** or **Salicyl-TPA-Ome** (0.1 mmol.) are solubilized in a mixture of ethanol/toluene mixture (1/1) (concentration  $\sim 1.75 \cdot 10^{-3}$  M), before the respective aniline (0.1 mmol. for 4-fluoro-aniline and 0.05 mmol. for 4-phenylenediamine) was added. The resulting mixture was stirred at 80°C for 2 hours in an oil bath, before it was transferred in an Eppendorf tube and centrifuged for 20 minutes. The resulting solid was washed with ethanol and pentane to give the desired product.

**Anil 3.** (yellow powder, 43 mg, 37%). Mp 211 – 218 °C.  $^1\text{H}$  NMR (500 MHz,  $\text{CD}_2\text{Cl}_2$ )  $\delta$  13.78 (s, 1H), 8.76 (s, 1H), 7.72 (d,  $^4J = 2.4$  Hz, 1H), 7.64 -7.58 (m, 3H), 7.52 (d,  $^3J = 8.7$  Hz, 2H), 7.38-7.32 (m, 2H), 7.32 -7.26 (m, 8H), 7.19-7.10 (m, 14H), 7.08-7.02 (m, 4H).  $^{13}\text{C}\{^1\text{H}\}$  NMR (126 MHz,  $\text{CD}_2\text{Cl}_2$ )  $\delta$  163.4, 158.1, 148.3, 148.3, 147.7, 147.6, 144.9, 134.6, 132.7, 132.4, 132.1, 130.8, 130.4, 129.8, 127.7, 125.0, 124.9, 124.6, 123.7, 123.5, 123.4, 123.3, 120.1, 116.9, 116.7.  $^{19}\text{F}$  NMR (471 MHz,  $\text{CD}_2\text{Cl}_2$ )  $\delta$  116.0. HRMS (ESI-TOF) m/z: [M+H] Calcd for  $\text{C}_{49}\text{H}_{37}\text{FN}_3\text{O}$ : 702.2915, Found: 702.2928. IR (neat):  $\nu = 3034, 1617, 1586, 1486, 1453, 1324, 1269, 1233, 1192, 1152, 831, 796, 749, 693, 507$   $\text{cm}^{-1}$ .

**Anil 4.** (yellow powder, 76 mg, 67%). Mp 238 – 243 °C.  $^1\text{H}$  NMR (500 MHz,  $\text{CDCl}_3$ )  $\delta$  13.83 (s, 1H), 8.71 (s, 1H), 7.66 (d,  $^4J = 2.4$  Hz, 1H), 7.55-7.50 (m, 3H), 7.41 (d,  $^3J = 8.7$  Hz, 2H), 7.32-7.27 (m, 2H), 7.15-7.07 (m, 10H), 7.04-6.98 (m, 4H), 6.87-6.82 (m, 8H), 3.81 (s, 12H).  $^{13}\text{C}\{^1\text{H}\}$  NMR (126 MHz,  $\text{CDCl}_3$ )  $\delta$  162.8, 162.7, 160.8, 157.4, 155.9, 148.0, 148.0, 144.4, 144.4, 141.1, 141.0, 132.3, 132.2, 130.2, 130.0, 129.5, 128.8, 127.1, 126.8, 126.6, 122.8, 122.7, 121.1, 120.3, 119.4, 116.5, 116.3, 114.8, 114.8, 55.6.  $^{19}\text{F}$  NMR (377 MHz,  $\text{CDCl}_3$ )  $\delta$  115.35. HRMS (ESI-TOF) m/z: [M+H] Calcd for  $\text{C}_{53}\text{H}_{45}\text{FN}_3\text{O}_5$ : 822.3338, Found: 822.3318. IR (neat):  $\nu = 3037, 2993, 2930, 2833, 1614, 1500, 1453, 1233, 1033, 826, 569$   $\text{cm}^{-1}$ .

**Anil 5.** (yellow powder, 142 mg, 81%). Mp 144 – 148 °C.  $^1\text{H}$  NMR (500 MHz,  $\text{CD}_2\text{Cl}_2$ )  $\delta$  14.53 (s, 1H), 8.77 (s, 1H), 7.64 (d,  $^4J = 2.3$  Hz, 1H), 7.61 (d,  $^3J = 8.6$  Hz, 2H), 7.57 (d,  $^4J = 2.3$  Hz, 1H), 7.53 (d,  $^3J = 8.6$  Hz, 2H), 7.32 (d,  $^3J = 8.9$  Hz, 2H), 7.30-7.24 (m, 8H), 7.18-7.08 (m, 12H), 7.08-7.00 (m, 4H), 6.71 (d,  $^3J = 8.9$  Hz, 2H), 3.40 (q,  $^3J = 7.1$  Hz, 4H), 1.18 (t,  $^3J = 7.1$  Hz, 6H).  $^{13}\text{C}\{^1\text{H}\}$  NMR (126 MHz,  $\text{CD}_2\text{Cl}_2$ )  $\delta = 157.8, 157.0, 148.1, 148.1, 147.9, 147.2, 147.1, 135.5, 134.8, 132.4, 131.7, 131.0,$

130.6, 129.8, 129.6, 128.7, 127.5, 124.8, 124.6, 124.5, 123.6, 123.2, 122.8, 120.5, 112.2, 44.9, 12.7. HRMS (ESI-TOF)  $m/z$ : [M+H] Calcd for  $C_{53}H_{47}N_4O$ : 755.3744, Found: 755.3717. IR (neat):  $\nu = 3033, 2968, 2927, 1616, 1587, 1509, 1486, 1448, 1265, 1177, 1073, 813, 748, 692, 505\text{ cm}^{-1}$ .

**Anil 6.** (yellow powder, 72 mg, 60%). Mp 115 – 124 °C (degradation).  $^1\text{H}$  NMR (500 MHz,  $\text{CDCl}_3$ )  $\delta$  14.59 (s, 1H), 8.72 (s, 1H), 7.59 (d,  $^4J = 2.3\text{ Hz}$ , 1H), 7.54 (d,  $^3J = 8.8\text{ Hz}$ , 2H), 7.48 (d,  $^4J = 2.3\text{ Hz}$ , 1H), 7.42 (d,  $^3J = 8.8\text{ Hz}$ , 2H), 7.29 (d,  $^3J = 9.0\text{ Hz}$ , 2H), 7.14 – 7.06 (m, 8H), 7.05 – 6.99 (m, 4H), 6.87 – 6.80 (m, 8H), 6.70 (d,  $^3J = 9.0\text{ Hz}$ , 2H), 3.81 (s, 6H), 3.80 (s, 6H), 3.40 (q,  $J = 7.0\text{ Hz}$ , 4H), 1.19 (t,  $J = 7.0\text{ Hz}$ , 6H).  $^{13}\text{C}\{^1\text{H}\}$  NMR (126 MHz,  $\text{CDCl}_3$ )  $\delta = 157.4, 156.9, 155.8, 155.8, 147.8, 147.7, 147.4, 141.2, 141.1, 135.6, 132.8, 131.7, 131.0, 130.1, 130.0, 129.9, 128.1, 127.1, 126.7, 126.5, 122.6, 121.3, 120.5, 120.1, 114.8, 114.7, 112.0, 55.6, 44.7, 12.7$ . HRMS (ESI-TOF)  $m/z$ : [M+H+] Calc. for  $C_{57}H_{55}N_4O_5$ : 875.4167, Found: 875.4133. IR (neat):  $\nu = 2928, 2831, 1612, 1499, 1451, 1233, 1176, 1031, 820, 571, 521\text{ cm}^{-1}$ .

**Bis-anil 7<sup>33</sup>** (yellow powder, 43 mg, 46%). Mp 216 – 220 °C (degradation).  $^1\text{H}$  NMR (400 MHz,  $\text{C}_2\text{D}_2\text{Cl}_4$ )  $\delta$  13.36 (bs, 2H), 8.84 (s, 2H), 7.76 -7.73 (m, 2H), 7.68-7.60 (m, 6H), 7.55-7.50 (m, 4H), 7.45 (s, 4H), 7.36-7.26 (m, 18H), 7.23-7.13 (m, 22H), 7.10-7.03 (m, 8H). HRMS (ESI-TOF)  $m/z$ : [M+H] Calcd for  $C_{92}H_{69}N_6O_2$ : 1289.5477, Found: 1289.5506. IR (neat):  $\nu = 3033, 1587, 1508, 1486, 1447, 1323, 1269, 1193, 1119, 1075, 839, 748, 693, 621, 508\text{ cm}^{-1}$ .

**Bis-anil 8** (yellow powder, 116 mg, 55%). Mp 148 – 152 °C (degradation).  $^1\text{H}$  NMR (500 MHz,  $\text{CDCl}_3$ )  $\delta$  13.88 (s, 2H), 8.79 (s, 2H), 7.67 (d,  $^4J = 2.2\text{ Hz}$ , 2H), 7.56-7.50 (m, 6H), 7.42 (dd,  $^3J = 8.7, ^4J = 2.2\text{ Hz}$ , 4H), 7.39 (s, 4H), 7.12 (dd,  $^3J = 8.9, ^4J = 2.2\text{ Hz}$ , 8H), 7.09 (dd,  $^3J = 8.9, ^4J = 2.2\text{ Hz}$ , 8H), 7.04-6.98 (m, 8H), 6.88-6.82 (m, 16H), 3.81 (s, 12H), 3.80 (s, 12H).  $^{13}\text{C}\{^1\text{H}\}$  NMR (126 MHz,  $\text{CDCl}_3$ )  $\delta$  155.9, 147.9, 141.0, 141.0, 132.2, 129.9, 129.4, 127.1, 126.7, 126.5, 122.4, 121.0, 120.2, 114.7, 114.7, 55.5. HRMS (ESI-TOF)  $m/z$ : [M+H] Calcd for  $C_{100}H_{85}N_6O_{10}$ : 1529.6322, Found: 1529.6278. IR (neat):  $\nu = 2952, 2831, 1606, 1500, 1453, 1317, 1235, 1177, 1104, 1029, 820, 726, 661, 582, 521\text{ cm}^{-1}$ .

#### General procedure for the synthesis of HBO 9 and 10

**Salicyl-TPA** or **Salicyl-TPA-OMe** (0.1 mmol.) and 2-aminophenol (0.14 mmol.) are dissolved in 15 mL of DMSO before potassium iodide (0.3 mmol) was added. The resulting mixture was stirred 3 hours at 110°C in an oil bath, before it was taken up in ethyl acetate, washed with water, dried on  $\text{MgSO}_4$  and the solvents removed *in vacuo*. The crude compounds were purified by chromatography on silica gel eluting with Pet. Ether/ $\text{CH}_2\text{Cl}_2$  7:3 to yield HBO 9 and 10.

**HBO 9.** (yellow powder, 78 mg, 68%). Mp 311 - 314 °C.  $^1\text{H}$  NMR (500 MHz,  $\text{C}_2\text{D}_2\text{Cl}_4$ )  $\delta$  12.12 (s, 1H), 8.24 (d,  $^4J = 2.3\text{ Hz}$ , 1H), 7.79 – 7.73 (m, 2H), 7.70 – 7.67 (m, 1H), 7.64 (d,  $^3J = 8.6\text{ Hz}$ , 2H), 7.58 (d,  $^3J = 8.6\text{ Hz}$ , 2H), 7.47 – 7.41 (m, 2H), 7.33 – 7.27 (m, 8H), 7.21 – 7.15 (m, 12H), 7.09 – 7.03 (m, 4H).  $^{13}\text{C}\{^1\text{H}\}$  NMR (126 MHz,  $\text{C}_2\text{D}_2\text{Cl}_4$ )  $\delta$  163.0, 154.7, 149.0, 147.4, 147.4, 146.8, 146.8, 139.6, 133.7, 132.6, 132.3, 131.1, 130.1, 129.9, 129.2, 128.0, 127.6, 127.3, 125.6, 125.1, 124.4, 124.2, 124.0,

123.6, 123.0, 122.9, 122.8, 119.1, 111.0, 110.7. HRMS (ESI-TOF) m/z: [M+H] Calcd for C<sub>49</sub>H<sub>35</sub>N<sub>3</sub>O<sub>2</sub>: 698.2756, Found: 698.2755. IR (neat):  $\nu$  = 3033, 2921, 1587, 1547, 1508, 1491, 1454, 1413, 1322, 1270, 1243, 1193, 1154, 1074, 830, 772, 744, 693, 320, 508 cm<sup>-1</sup>.

**HBO 10.** (yellow powder, 18 mg, 16%). Mp 270 - 274 °C. <sup>1</sup>H NMR (500 MHz, CDCl<sub>3</sub>)  $\delta$  11.98 (s, 1H), 8.18 (d, <sup>4</sup>J = 2.4 Hz, 1H), 7.74-7.69 (m, 2H), 7.65-7.61 (m, 1H), 7.55 (d, <sup>3</sup>J = 8.7 Hz, 2H), 7.48 (d, <sup>3</sup>J = 8.7 Hz, 2H), 7.42-7.37 (m, 2H), 7.15-7.07 (m, 8H), 7.03 (d, <sup>3</sup>J = 8.7 Hz, 4H), 6.85 (d, <sup>3</sup>J = 8.7 Hz, 8H). <sup>13</sup>C{<sup>1</sup>H} NMR (126 MHz, CDCl<sub>3</sub>)  $\delta$  163.5, 156.0, 156.1, 155.1, 149.3, 148.2, 148.1, 141.1, 140.1, 132.7, 132.7, 132.3, 130.5, 130.1, 129.6, 127.3, 126.9, 126.6, 125.6, 125.2, 123.5, 121.2, 120.2, 119.4, 114.9, 114.8, 111.1, 110.8, 55.7. HRMS (ESI-TOF) m/z: [M+H] Calcd for C<sub>53</sub>H<sub>44</sub>N<sub>3</sub>O<sub>6</sub>: 818.3225, Found: 818.3219. IR (neat):  $\nu$  = 2931, 2835, 1604, 1498, 1453, 1318, 1275, 1231, 1193, 1103, 1032, 824, 743, 572, 524 cm<sup>-1</sup>.

#### **Second procedure for the synthesis of HBO 10.**

**Salicyl-TPA-OMe** (0.1 mmol.) and 2-aminophenol (0.14 mmol.) are dissolved in 20 mL of MeOH/DMSO (9:1, v/v) before potassium cyanide (0.1 mmol) and phenyl boronic acid (0.01 mmol.) were added. The resulting mixture was stirred 3 hours at room temperature before it was taken up in ethyl acetate, washed with water, dried on MgSO<sub>4</sub> and the solvents removed *in vacuo*. The crude compounds were purified by chromatography on silica gel eluting with Pet. Ether/CH<sub>2</sub>Cl<sub>2</sub> 7:3 to yield **HBO 10** (yellow powder, 41 mg, 46%). Mp 270 - 274 °C. <sup>1</sup>H NMR (500 MHz, CDCl<sub>3</sub>)  $\delta$  11.98 (s, 1H), 8.18 (d, <sup>4</sup>J = 2.4 Hz, 1H), 7.74-7.69 (m, 2H), 7.65-7.61 (m, 1H), 7.55 (d, <sup>3</sup>J = 8.7 Hz, 2H), 7.48 (d, <sup>3</sup>J = 8.7 Hz, 2H), 7.42-7.37 (m, 2H), 7.15-7.07 (m, 8H), 7.03 (d, <sup>3</sup>J = 8.7 Hz, 4H), 6.85 (d, <sup>3</sup>J = 8.7 Hz, 8H). <sup>13</sup>C{<sup>1</sup>H} NMR (126 MHz, CDCl<sub>3</sub>)  $\delta$  163.5, 156.0, 156.1, 155.1, 149.3, 148.2, 148.1, 141.1, 140.1, 132.7, 132.7, 132.3, 130.5, 130.1, 129.6, 127.3, 126.9, 126.6, 125.6, 125.2, 123.5, 121.2, 120.2, 119.4, 114.9, 114.8, 111.1, 110.8, 55.7. HRMS (ESI-TOF) m/z: [M+H] Calcd for C<sub>53</sub>H<sub>44</sub>N<sub>3</sub>O<sub>6</sub>: 818.3225, Found: 818.3219. IR (neat):  $\nu$  = 2931, 2835, 1604, 1498, 1453, 1318, 1275, 1231, 1193, 1103, 1032, 824, 743, 572, 524 cm<sup>-1</sup>.

#### **ASSOCIATED CONTENT:**

##### **• Data Availability Statement**

The data underlying this study are available in the published article and its Supporting Information.

##### **• Supporting Information Statement**

<sup>1</sup>H and <sup>13</sup>C NMR spectra, spectroscopic data, HR-MS spectra, DLS analysis and details of the computational procedures and methods.

#### **Acknowledgments**

The authors thank the CNRS for financial support. T.S. acknowledges the ministère de l'enseignement supérieur et de la recherche for a PhD fellowship. This work of the Interdisciplinary Institute

HiFunMat, as part of the ITI 2021-2028 program of the University of Strasbourg, CNRS and Inserm, was supported by IdEx Unistra (ANR-10-IDEX-0002) and SFRI (STRAT'US project, ANR-20-SFRI-0012) under the framework of the French Investments for the Future Program. D.J. and A.D.L. thank the CCIPL (*Centre de Calcul Intensif des Pays de la Loire*) installed in Nantes for generous allocation of computational time.

## References

- (1) (a) Zhao, J.; Ji, S.; Chen, Y.; Guo, H.; Yang, P. Excited state intramolecular proton transfer (ESIPT): from principal photophysics to the development of new chromophores and applications in fluorescent molecular probes and luminescent materials. *Phys. Chem. Chem. Phys.*, **2012**, 14, 8803-8817. (b) Massue, J.; Jacquemin, D.; Ulrich, G. Molecular Engineering of Excited-state Intramolecular Proton Transfer (ESIPT) Dual and Triple Emitters. *Chem. Lett.*, **2018**, 47, 9, 1083-1089. (c) Liu, Z.-Y.; Hu, J.-W.; Huang, T.-H.; Chen, K.-Y.; Chou, P.-T. Excited-state intramolecular proton transfer in the kinetic-control regime. *Phys. Chem., Chem. Phys.*, **2020**, 22, 22271-22278. (d) Liu, Z.-Y.; Hu, J.-W.; Chen, C.-L.; Chen, Y.-A.; Chen, K.-Y.; Chou, P.-T. Correlation among Hydrogen Bond, Excited-State Intramolecular Proton-Transfer Kinetics and Thermodynamics for -OH Type Proton-Donor Molecules. *J. Phys. Chem. C*, **2018**, 122, 38, 21833-21840.
- (2) (a) Kaur, I.; Shivani; Kaur, P.; Singh, K. 2-(2'-Hydroxyphenyl)benzothiazole derivatives: Emission and color tuning. *Dyes Pigm.*, **2020**, 176, 108198. (b) Göbel, D.; Rusch, P.; Duvinage, D.; Stauch, T.; Bigall, N.C.; Nachtsheim, B.J. Substitution Effect on 2-(Oxazoliny)-phenols and 1,2,5-Chalcogenadiazole-Annulated Derivatives: Emission-Color-Tunable, Minimalistic Excited-State Intramolecular Proton Transfer (ESIPT)- Based Luminophores. *J. Org. Chem.*, **2021**, 86, 14333-14355. (c) Zhang, M.; Cheng, R.; Lan, J.; Zhang, H.; Yan, L.; Pu, X.; Huang, Z.; Wu, D.; You, J. Oxidative C-H/C-H Cross-Coupling of [1,2,4]Triazolo[1,5- a]pyrimidines with Indoles and Pyrroles: Discovering Excited-State Intramolecular Proton Transfer (ESIPT) Fluorophores. *Org. Lett.*, **2019**, 21, 4058-4062.
- (3) (a) Kwon, J.E.; Park, S.Y. Advanced Organic Optoelectronic Materials: Harnessing Excited-State Intramolecular Proton Transfer (ESIPT) Process. *Adv. Mater.*, **2011**, 23, 32, 3615-3642. (b) Mamada, M.; Inada, K.; Komino, T.; Potscavage, Jr.; W.J.; Nakanotani, H.; Adachi, C. Highly Efficient Thermally Activated Delayed Fluorescence from an Excited-State Intramolecular Proton Transfer System. *ACS Central Sci.*, **2017**, 3, 7, 769. (c) Zhang, Z.; Chen, Y.-A.; Hung, W.-Y.; Tang, W.-F.; Hsu, Y.-H.; Chen, C.-L.; Meng, F.-Y.; Chou, P.-T. Control of the Reversibility of Excited-State Intramolecular Proton Transfer (ESIPT) Reaction: Host-Polarity Tuning White Organic Light Emitting Diode on a New Thiazolo[5,4-d]thiazole ESIPT System. *Chem. Mater.*, **2016**, 28, 23, 8815-8824. (d) Wu, K.; Zhang, T.; Wang, Z.; Wang, L.; Zhan, L.; Gong, S.; Zhong, C.; Lu, Z.-H.; Zhang, S.;

Yang, C. De Novo Design of Excited-State Intramolecular Proton Transfer Emitters via a Thermally Activated Delayed Fluorescence Channel. *J. Am. Chem. Soc.* **2018**, 140, 28, 8877-8886.

(4) (a) Tian, J.; Shi, D.; Zhang, Y.; Li, X.; Li, X.; Teng, H.; James, T.D.; Li, J.; Guo, Y. Stress response decay with aging visualized using a dual-channel logic-based fluorescent probe. *Chem. Sci.*, **2021**, 12, 40, 13483-13491. (b) Ren, H.; Huo, F.; Wu, X.; Liu, X.; Yin, C. An ESIPT-induced NIR fluorescent probe to visualize mitochondrial sulfur dioxide during oxidative stress in vivo. *Chem. Commun.*, **2021**, 57, 655-658.

(5) (a) Wu, L.; Wang, Y.; Weber, M.; Liu, L.; Sedgwick, A.C.; Bull, S.D.; Huang, C.; James, T.D. ESIPT-based ratiometric fluorescence probe for the intracellular imaging of peroxynitrite. *Chem. Commun.*, **2018**, 54, 9953-9956. (b) Wu, L.; Liu, L.; Han, H.-H.; Tian, X.; Odyniec, M.L.; Feng, L.; Sedgwick, A.C.; He, X.-P.; Bull, S.D.; James, T.D. ESIPT-based fluorescence probe for the ratiometric detection of superoxide. *New J. Chem.*, **2019**, 43, 2875-2877. (c) Devi, M.; Sharma, P.; Kumar, A.; Kaur, S.; Kumar, M.; Bhalla, V. ESIPT Active Assemblies for 'On-On' Detection, Cell Imaging and Hampering Cellular Activity of 2,6-Dichloro-4-nitroaniline. *Chem. Asian J.*, **2022**, 17, 4, e202101219.

(6) Zhang, Y.; Yang, H.; Ma, H.; Bian, G.; Zang, Q.; Sun, J.; Zhang, C.; An, Z.; Wang, W.-Y. Excitation Wavelength Dependent Fluorescence of an ESIPT Triazole Derivative for Amine Sensing and Anti-Counterfeiting Applications. *Angew. Chem., Int. Ed.*, **2019**, 58, 8773-8778.

(7) Hu, H.; Cheng, X.; Ma, Z.; Sijbesma, R.P.; Ma, Z. Polymer Mechanochromism from Force-Tuned Excited-State Intramolecular Proton Transfer. *J. Am. Chem. Soc.*, **2022**, 144, 22, 9971.

(8) Berbigier, F.G.; Duarte, L.G.T.A.; Fialho Zawacki, M.; de Araújo, B.B.; de Moura Santos, C.; Atvars, T.D.Z.; Gonçalves, P.F.B.; Petzhold, C.L.; Rodembusch, F.S. ATRP Initiators Based on Proton Transfer Benzazole Dyes: Solid-State Photoactive Polymer with Very Large Stokes Shift. *ACS Appl. Polym. Mater.*, **2020**, 2, 1406-1416.

(9) (a) Padalkar, V.S.; Seki, S. Excited-state intramolecular proton-transfer (ESIPT)-inspired solid state emitters. *Chem. Soc. Rev.*, **2016**, 45, 169-202. (b) Chen, L.; Fu, P.-Y.; Wang, H.-P.; Pan, M. Excited-State Intramolecular Proton Transfer (ESIPT) for Optical Sensing in Solid State. *Adv. Opt. Mater.*, **2021**, 9, 23, 2001952.

(10) (a) Zhao, Z.; Zhang, H.; Lam, J.W.Y.; Tang, B.Z. Aggregation-Induced Emission: New Vistas at the Aggregate Level. *Angew. Chem., Int. Ed.*, **2020**, 59, 9888-9907. (b) Suman, G.R.; Pandey, M.; Chakravarthy, J. Review on new horizons of aggregation induced emission: from design to development. *Mat. Chem. Front.*, **2021**, 5, 4, 1541-1584. (c) Peng, Q.; Shuai, Z. Molecular mechanism of aggregation-induced emission. *Aggregate*, **2021**, 2, 5, e91.

(11) (a) Feng, H.-T.; Yuan, Y.-X.; Xiong, J.-B.; Zheng, Y.-S.; Tang, B.Z. Macrocycles and cages based on tetraphenylethylene with aggregation-induced emission effect. *Chem. Soc. Rev.*, **2018**, 47, 7452-7476. (b) La, D.D.; Bhosale, S.V.; Jones, L.A.; Bhosale, S.V. Tetraphenylethylene-Based AIE-Active Probes for Sensing Applications. *ACS Appl. Mater. Interfaces*, **2018**, 10, 12189-12216.

- (12) Jana, P.; Kanva, S. Aggregation-Induced Emission and Organogels with Chiral and Racemic Pyrene-Substituted Cyanostyrenes. *Langmuir*, **2020**, 36, 10, 2720-2728.
- (13) (a) He, B.; Huang, J.; Zhang, J.; Sung, H.H.Y.; Lam, J.W.Y.; Zhang, Z.; Yan, S.; Wang, D.; Zhang, J.; Tang, B.Z. Novel Quinolizine AIE System: Visualization of Molecular Motion and Elaborate Tailoring for Biological Application. *Angew. Chem., Int. Ed.*, **2022**, 61, 11, e202117709. (b) Shen, P.; Zhuang, Z.; Zhao, Z.; Tang, B.Z. AIEgens based on main group heterocycles. *J. Mater. Chem. C*, **2018**, 6, 11835-11852.
- (14) (a) Massue, J.; Felouat, A.; Curtil, M.; Vérité, P.M.; Jacquemin, D.; Ulrich, G. Solution and Solid-State Excited-State Intramolecular Proton Transfer (ESIPT) emitters incorporating Bis-triethyl- or triphenylsilylethynyl units. *Dyes Pigm.*, **2019**, 160, 915-922. (b) Takagi, K.; Ito, K.; Yamada, Y.; Nakashima, T.; Fukuda, R.; Ehara, M.; Masu, H. Synthesis and Optical Properties of Excited-State Intramolecular Proton Transfer Active  $\pi$ -Conjugated Benzimidazole Compounds: Influence of Structural Rigidification by Ring Fusion. *J. Org. Chem.* **2017**, 82, 12173-12180.
- (15) (a) Pariat, T.; Stoerkler, T.; Diguët, C.; Laurent, A.D.; Jacquemin, D.; Ulrich, G.; Massue, J. Dual Solution-/Solid-State Emissive Excited-State Intramolecular Proton Transfer (ESIPT) Dyes: A Combined Experimental and Theoretical Approach. *J. Org. Chem.*, **2021**, 86, 17606-17619. (b) Stoerkler, T.; Laurent, A.D.; Ulrich, G.; Jacquemin, D.; Massue, J. Influence of ethynyl extension on the dual-state emission properties of pyridinium-substituted ESIPT fluorophores. *Dyes Pigm.*, **2022**, 208, 110872.
- (16) (a) Huang, M.; Zhou, J.; Xu, K.; Zhu, X.; Wan, Y. Enhancement of the excited-state intramolecular proton transfer process to produce all-powerful DSE molecules for bridging the gap between ACQ and AIE. *Dyes Pigm.*, **2019**, 160, 839-847. (b) Huber, A.; Dubbert, J.; Scherz, T.D.; Voskuhl, J. Design Concepts for Solution and Solid-State Emitters—A Modern View point on Classical and Non-Classical Approaches. *Chem. Eur. J.*, **2023**, 29, e2022024. (c) Belmonte-Vazquez, J.L.; Amador-Sanchez, Y.A.; Rodriguez-Cortes, L.A.; Rodriguez-Molina, B. Dual-State Emission (DSE) in Organic Fluorophores: Design and Applications. *Chem. Mater.*, **2021**, 33, 7160-7184.
- (17) Azarias, C.; Budzák, S.; Laurent, A.D.; Ulrich, G.; Jacquemin, D. Tuning ESIPT fluorophores into dual emitters. *Chem. Sci.*, **2016**, 120, 3763-3774.
- (18) (a) Demchenko, A.P.; Tang, K.-C.; Chou, P.-T. Excited-state proton coupled charge transfer modulated by molecular structure and media polarization. *Chem. Soc. Rev.*, **2013**, 42, 1379-1408. (b) Munch, M.; Colombain, E.; Stoerkler, T.; Vérité, P.M.; Jacquemin, D.; Ulrich, G.; Massue, J. Blue-Emitting 2-(2'-Hydroxyphenyl)benzazole Fluorophores by Modulation of Excited-State Intramolecular Proton Transfer: Spectroscopic Studies and Theoretical Calculations. *J. Phys. Chem. B*, **2022**, 126, 2108-2118.
- (19) Sakai, K.-I.; Ishikawa, T.; Akutagawa, T. A blue-white-yellow color-tunable excited state intramolecular proton transfer (ESIPT) fluorophore: sensitivity to polar-nonpolar solvent ratios. *J. Mater. Chem. C*, **2013**, 1, 47, 7866-7871.

- (20) (a) Gayathri, P.; Pannipara, M.; Al-Sehemi, A.G.; Anthony, S.P. Recent advances in excited state intramolecular proton transfer mechanism-based solid state fluorescent materials and stimuli-responsive fluorescence switching. *CrystEngComm.*, **2021**, 23, 3771-3789. (b) Sedgwick, A.C.; Wu, L.; Han, H.-H.; Bull, S.D.; He, X.-P.; James, T.D.; Sessler, J.L.; Tang, B.Z.; Tian, H.; Yoon, J. Excited-state intramolecular proton-transfer (ESIPT) based fluorescence sensors and imaging agents. *Chem. Soc. Rev.*, **2018**, 47, 8842-8880. (c) Alam, P.; Kachwal, V.; Laska, I.R. A multi-stimuli responsive "AIE" active salicylaldehyde-based Schiff base for sensitive detection of fluoride. *Sens. Actuators B: Chem.*, **2016**, 228, 539-550. (d) Xie, H.; Li, Z.; Gong, J.; Hu, L.; Alam, P.; Ji, X.; Hu, Y.; Chau, J.H.C.; Lam, J.W.Y.; Kwok, R.T.K.; Tang, B.Z. Phototriggered Aggregation-Induced Emission and Direct Generation of 4D Soft Patterns. *Adv. Mater.*, **2021**, 33, 2105113.
- (21) Stoerkler, T.; Retailleau, P.; Jacquemin, D.; Ulrich, G.; Massue, J. Heteroaryl-Substituted bis-Anils: Aggregation-Induced Emission (AIE) Derivatives with Tunable ESIPT Emission Color and pH Sensitivity. *Chem. Eur. J.*, **2023**, 29, 14, e202203766.
- (22) Gayathri, P.; Pannipara, M.; Al-Sehemi, A.G.; Anthony, S.P. Triphenylamine-based stimuli-responsive solid-state fluorescent materials. *New J. Chem.*, **2020**, 44, 8680-8696.
- (23) Zhang, Q.; Li, Y.; Cao, Z.; Zhu, C. Aggregation-induced emission spectra of triphenylamine salicylaldehyde derivatives via excited-state intramolecular proton transfer revealed by molecular spectral and dynamics simulations. *RSC Adv.*, **2021**, 11, 37171-37180.
- (24) Yin, W.; Li, Y.; Li, N.; Yang, W.; An, H.; Gao, J.; Bi, Y.; Zhao, N. Hybridization of Triphenylamine and Salicylaldehyde: A Facile Strategy to Construct Aggregation-Induced Emission Luminogens with Excited-State Intramolecular Proton Transfer for Specific Lipid Droplets and Gram-Positive Bacteria Imaging. *Adv. Optical Mater.* **2020**, 1902027.
- (25) (a) Mishra, V.R.; Ghanavatkar, C.W.; Sekar, N. Towards NIR-Active Hydroxybenzazole (HBX)-Based ESIPT Motifs: A Recent Research Trend. *ChemistrySelect*, **2020**, 5, 2103-2113. (b) Chen, Y.; Fang, Y.; Gu, H.; Qiang, J.; Li, H.; Fan, J.; Cao, J.; Wang, F.; Lu, S.; Chen, X. Color-Tunable and ESIPT-Inspired Solid Fluorophores Based on Benzothiazole Derivatives: Aggregation-Induced Emission, Strong Solvatochromic Effect, and White Light Emission. *ACS Appl. Mater. Interfaces*, **2020**, 12, 49, 55094-55106.
- (26) Pariat, T.; Munch, M.; Durko-Maciag, M.; Mysliwiec, J.; Retailleau, P.; V  rit  , P.M. ; Jacquemin, D.; Massue, J.; Ulrich, G. Impact of Heteroatom Substitution on Dual-State Emissive Rigidified 2-(2'-hydroxyphenyl)benzazole Dyes: Towards Ultra-Bright ESIPT Fluorophores. *Chem. Eur. J.*, **2021**, 27, 10, 3483-3495.
- (27) (a) Guieu, S.; Cardona, F.; Rocha, J.; Silva, A.M.S. Tunable Color of Aggregation-Induced Emission Enhancement in a Family of Hydrogen-Bonded Azines and Schiff Bases. *Chem. Eur. J.*, **2018**, 24, 17262. (b) Frath, D.; Benelhadj, K.; Munch, M.; Massue, J.; Ulrich, G. Polyanils and Polyboranils: Synthesis, Optical Properties, and Aggregation-Induced Emission. *J. Org. Chem.*, **2016**, 81, 9658.

- (28) Christiansen, O.; Koch, H.; Jørgensen, P. The Second-Order Approximate Coupled Cluster Singles and Doubles Model CC2. *Chem. Phys. Lett.* **1995**, 243, 409-418.
- (29) Adamo, C.; Jacquemin, D. The calculations of Excited-State Properties with Time-Dependent Density Functional Theory. *Chem. Soc. Rev.* **2013**, 42, 845-856.
- (30) Vérité, P.M.; Guido, C.A.; Jacquemin, D. First-Principles Investigation of the Double ESIPT Process in a Thiophene-Based Dye. *Phys. Chem. Chem. Phys.* **2019**, 21, 2307-2317.
- (31) Changa, Y.J.; Chow, T.J. Triaryl linked donor acceptor dyads for high-performance dye-sensitized solar cells. *Tetrahedron Lett.*, **2009**, 65, 9626-9632.
- (32) Schlüter, F.; Riehemann, K.; Kehr, N.S.; Quici, S.; Daniliuc, C.G.; Rizzo, F. A highly fluorescent water soluble spirobifluorene dye with a large Stokes shift: synthesis, characterization and bio-applications. *Chem. Commun.*, **2018**, 54, 642-645.
- (33) A  $^{13}\text{C}$  NMR spectrum was not obtained due to inherent low solubility.